



Double-Container Gas Fuel Control Valve: Numerical Analysis and Operating Conditions

S. Zirak^{1†}, M. Seifi² and A. Ramesh²

¹ Mechanical Engineering Department, Semnan University, Semnan, Semnan, 35131-19111, Iran

² MAPNA Turbine Engineering & Manufacturing Co. (TUGA), Karaj, Alborz, 15875-5643, Iran

†Corresponding Author Email: s_zirak@semnan.ac.ir

(Received February 2, 2019; accepted April 23, 2019)

ABSTRACT

Flow behavior through a gas turbine double-container fuel valve is numerically studied. Normally the gas fuel supply pressure of the gas turbine sites is over 20+ barg while the combustion chamber pressure is around 12 barg in base load operation and slightly more than atmospheric during start-up. Therefore, the flow control through this high range of pressure ratios is a very difficult and costly task with a single-container control valve. The double-container valve is an innovative design which consists of two parts, SRV (Stop Ratio Valve) followed by GCV (Gas Control Valve), in a compact unit. SRV maintains a significantly low pressure upstream of the GCV during gas turbine firing to establish flame and control fuel flow during acceleration. It opens the GCV to a position where it is much easier to control the flow through the valve. The same situation exists in base load operation when the turbine load is changing. The obtained results prove the special design of the valve to maintain linear characteristics of flow with stroke position in GCV. The results of the mass flow are given for various GCV stroke openings at various valve pressure ratios. Also, the range of pressure ratios for a proper operation of GCV is determined. SRV regulates the middle pressure between the two parts based on rotor speed. Therefore, a sensitive combination of globes position takes place during gas turbine operation.

Keywords: Double-container; Control valve; Gas turbine; Gas fuel; Numerical analysis; Operating conditions.

NOMENCLATURE

A	equivalent mass flow	ε	turbulence rate of dissipation
$C_1, C_2, C_{2\infty}$	model constants	μ	dynamic viscosity
$C_\mu, C_{\mu\infty}$	model constants	μ_t	turbulent viscosity
i, j, l	direction	ν	kinematic viscosity
k	turbulence kinetic energy	ρ	density
P_0	total pressure	σ_ε	turbulent Prandtl number for ε
R_t	turbulent Reynolds number	σ_k	turbulent Prandtl number for k
T_0	total temperature		
U	velocity		

1. INTRODUCTION

A double-container valve controls gas fuel flow to the can-annular combustion chambers of the industrial gas turbine. The valve is mounted on turbine gas skid before fuel nozzle of the combustion chambers. The valve regulates the mass flow of the gas to the turbine at various turbine operating conditions. Normally, the pressure of the

supply line in the gas turbine sites is +20 in bars. This is while the maximum pressure in the combustion chamber is around 12 barg in the normal operation. It means a too high pressure ratio across the valve during start-up in which the combustion chamber pressure is slightly more than atmospheric. The same condition is experienced in base load operation when the turbine load is changing. This causes difficulties for achieving a

linear valve characteristic with customary single-container valves. The linear characteristic, which is important during the turbine starting and acceleration and also in rated speed, refers to a linear relation of gas flow rate with valve stroke position.

Figure 1 represents a schematic diagram of a double-container valve; it consists of a primary stop/ratio valve (SRV), the left part, followed by a secondary gas control valve (GCV), both in a compact unit. SRV provides a dual function; one function rapidly shuts off fuel, another purpose is to limit pressure upstream of GCV so that the flow through the GCV is proportional to the opening ("stroke") of the valve.

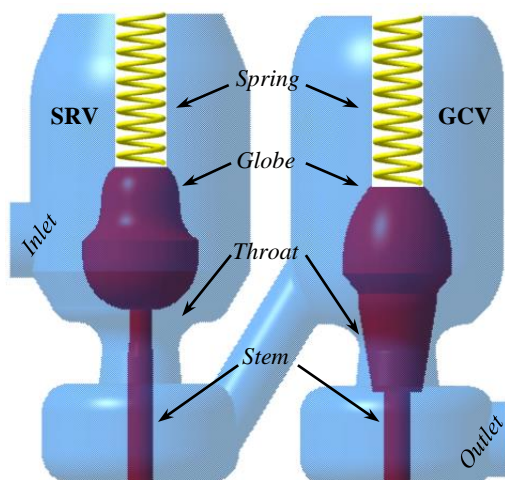


Fig. 1. Schematic of double-container gas fuel control valve, SRV (left) and GCV (right).

In a recent medium duty gas turbine, the unit is started-up in approximately twelve minutes (Zirak, Ebrahimi, & Maissamy, 2015). During the turbine acceleration, the pressure required at the fuel nozzle is about a fraction of one barg. If exists a single plug control valve, it should be open some millimeters and its reliability is severely limited, and hence, establishing flame is very difficult. The SRV maintains an approximately 2.0 bar pressure difference across GCV by increasing the intermediate pressure (downstream of SRV and upstream to GCV) as a function of turbine speed until the turbine reaches to full speed no-load (FSNL). During firing (establishing flame in the combustors), the GCV can be opened to a position where it is much easier to control the flow through the valve. The same is true for the acceleration of the turbine to rated speed. When the turbine is synchronized and loaded, the GCV opens to increase fuel flow to the combustors. This increase of fuel flow tends to cause the pressure upstream of the GCV to drop, but the SRV will open slightly to maintain the pressure reference as the GCV is opened. As the load is reduced, the GCV closes and the pressure upstream of the GCV tends to increase, but the SRV closes slightly to maintain the pressure

reference as the GCV is closed. So, the pressure downstream of the GCV will change as the unit is loaded and unloaded and started and accelerated (and decelerated). The SRV moves to whatever position is required to try to maintain the pressure upstream of the GCV equal to the pressure reference which is a function of turbine speed. Also, if the gas pressure of the supply line increases during steady-state turbine operation, the pressure upstream to the GCV would tend to increase, but the SRV will close slightly to maintain the pressure equal to the reference. In a case of supply line pressure much lower than it should be, the SRV is at 100% stroke (full open), and usually, the power output of the turbine is also lower than the design value.

At the present time, there are single valves which could have been used instead of double-container, but those valves could be extremely expensive and very difficult to interface with. Therefore, some turbine manufacturer probably decided to use double-container in order to reduce the complexity of the control system.

The present paper aims to numerically investigate various SRV and GCV strokes configurations during turbine operation and calculates the fuel flow rate. Also, it investigates the possible range of pressure ratios in which the GCV can operate properly. These data are necessary for the design of the turbine control system.

There are several researches showing the ability of computational fluid dynamics (CFD) to represent flow field through different models of controlling valves. Davis and Stewart (2002a) evaluated the use of CFD tool in industrial applications by performing an axisymmetric simulation inside the primary globe control valve to obtain pressure drop and flow field. Their model can predict pressure drop at different globe states except the fully open, therefore, the flow coefficient, C_v , can be calculated. In the second part of the work (Davis & Stewart, 2002b), they verified the CFD results of globe control valve model with experiments. They showed that the axisymmetric numerical model accurately solves an axisymmetric flow field. Amirante, Del Vescovo, & Lippolis (2006a) performed a complete numerical analysis to evaluate the driving force acting on a 4/3 hydraulic open center directional control valve spool. They used FLUENT code and compared the results with those of experimental which obtained by the same authors in previous research (Amirante, Del Vescovo, & Lippolis, 2006b). The obtained numerical results showed an important difference between an open center valve and a closed center one. Morita *et al.* (2007) performed both experiments and CFD calculations for a partially open steam control valve which causes large vibrations in the piping system of a power plant. They observed, under the middle-opening condition, a complex 3-dimensional flow structure sets up in the valve region leading to a high pressure region on a part of the valve body. This region rotates circumferentially, causes a cyclic asymmetric side load, and finally causes

system vibrations. [Amirante *et al.* \(2007\)](#) used the abilities of the Fluent software to analyze the flow field through a proportional valve. They investigated the features to reduce the required force necessary to keep open the valve. They showed a very good agreement between Fluent numerical results and manufacture catalog data for valve flow rate versus stroke opening. These computations indicated that the unbalanced flow forces on the spool could be reduced by optimizing the internal structural profile of the valve. [Beune *et al.* \(2012\)](#) used an incompressible transient CFD model to analyze the opening characteristics of high pressure safety valves. They applied the commercial ANSYS CFX code with Fluid-Structure Interaction (FSI). They explained that the use of FSI indicates some aspects of the flow that cannot be observed by a steady state approach. They also showed that in the high pressure flow condition, the real-gas characteristics become more apparent and cause a decreasing force when the valve open, therefore, the rate of pressure increase at the valve inlet becomes more important. [Chattopadhyay *et al.* \(2012\)](#) investigated flow behavior in a pressure regulating valve using ANSYS FLUENT package. They solved viscous compressible flow at various valve opening and pressure drop. They initially used the standard k- ϵ model, and predict higher levels of turbulent kinetic energy, finally adopted the realizable k- ϵ model for turbulence closure. [Peng *et al.* \(2012\)](#) used FLUENT to simulate the flow through a double-nozzle flapper main valve and servo valve. The simulation was for the main valve spool on a certain position. They made some improvement to the main valve core. [Lisowski *et al.* \(2013\)](#) numerically solved the flow field of a continual produced directional control valve to investigate the effect of increasing the flow range on spool flow forces. They calculated pressure and viscous forces by means of a 3D CFD model. The obtained results from CFD were compared with those from test bench data and the accuracy of the method has been verified. [Song *et al.* \(2014\)](#) numerically investigated fluid and dynamic characteristics of a safety relieve valve using ANSYS CFX computational code with moving mesh technique. They obtained the details of compressible flow through the valve together with analyzing disc motion and forces on the disc. [Qian *et al.* \(2014\)](#) analyzed flow dynamics inside a new type pilot-control globe valve which needs low driving energy consumption. They used a mathematical model parallel with numerical analysis to verify the working principle of the valve. They related inlet static pressure to the valve core's displacement to reduce the design process for further optimization. [Fang and Singh \(2015\)](#) analyzed the flow field through the valve lift located upstream of an internal combustion engine by CFD methods. The experiment showed that in certain cases the flow rate is decreased by increasing in valve lift although it thought that the mass flow always should be increased with valve lift increase. It was due to flow separation at the valve seat. It was not easy to solve that by

common CFD analyses, but they showed that using a dense mesh around the valve seat can predict the real configuration of the separated region. They performed the commercial CONVERGE CFD code in their work. [Wu *et al.* \(2015\)](#) tried to show the power of CFD in analyzing the flow of pressure control valves. They selected a spring load valve which its opening is under the influence of inlet and outlet pressure and also the flow rate. They performed direct CFD simulations together with indirect CFD method. The results of both methods showed a good agreement with the data gathered from conducted experiments. [Jin *et al.* \(2016\)](#) investigated the choked flow of an introduced high multi-stage pressure reduction valve using FLUENT code. In order to verify the applicability of the recommended valve, the flow characteristics of two fluids, superheated steam and hydrogen, under different valve opening was carried out. [Lisowski and Filo \(2016\)](#) analyzed the flow field through a proportional flow valve by CFD method for two types of spool opening, round and triangular. They analyzed the flow for the Reynolds number ranging from 500 to 4200, corresponding to transitional and partially turbulent flow. They used the commercial ANSYS Fluent software with the k-epsilon turbulent modeling. The comparison of the numerical results of flow rate with test data showed a good agreement. [Jin *et al.* \(2017\)](#) analyzed the pressure drop through Pilot-Control Globe Valves (PCGVs) with various structures by an implementation of CFD. Numerical solutions were compared with experiments. Although a simplified model of the original valve was considered, the accuracy of numerical solutions was proved. As a result, it proposed straightforward guidance to design PCGVs based on spring stiffness and dimension of structural parameters. [Qian *et al.* \(2017\)](#) numerically studied the compressible superheated steam flow characteristics inside a proposed pressure reducing valve of the piping systems. Comparison with experimental results showed an agreement and both of them confirmed the linear flow rate characteristic of the valve. [Saha *et al.* \(2014\)](#) investigated flow characteristics inside a pressure regulating and shut-off valve (PRSOV) by means of CFD (Ansys Fluent) and 2D modeling. The working fluid in their research was air as a compressible domain. The valve outlet pressure was intended to set on an almost fixed value, and this study was to find the spool position when the inlet pressure is changed within a wide range. To achieve this goal, they used a dynamic mesh and developed a special function that using force balance approach to calculate flow force on the spool, its movement, and final position.

The above-mentioned researches show the capability and continual use of CFD methods to determine flow characteristics of different valve types by researchers. Therefore, in the present paper, the numerical 3D analysis of the gas flow through the double-container gas fuel control valve is presented.

2. NUMERICAL METHOD AND BOUNDARY CONDITIONS

The flow domain is the internal passage of a double-globe flow valve. The only available geometry sheet is a two-dimensional drawing. In this respect, there could be some uncertainties in gathering the geometry data. Figure 2 shows the 3-D model of the valve. Flow analysis is performed first for separate SRV and GCV, and second, for both valves in a compact unit.

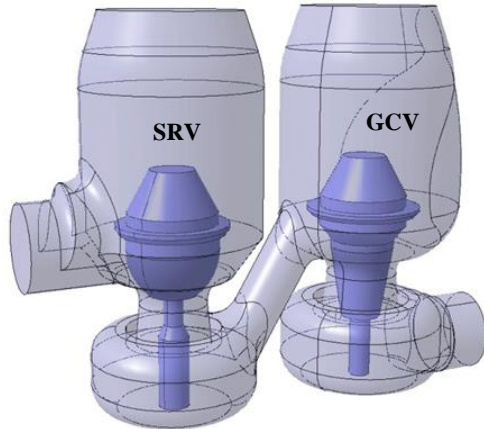


Fig. 2. 3-D model of SRV (left) and GCV (right).

A 3-D finite volume solver is used to simulate the viscous compressible flow of gas through the valves. Normally, the valve geometry is such that the low Reynolds number flows is rarely formed even for very low flow rates through the valve, and therefore, the standard k- ϵ turbulence model gives reasonable results. Launder and Spalding (1974) express a version of the model for low Reynolds number flows, in which turbulence kinetic energy, k, and turbulence dissipation rate, ϵ , are determined from the following pair of equations:

$$\begin{aligned} \frac{Dk}{Dt} &= \frac{1}{\rho} \frac{\partial}{\partial x_j} \left[\left(\frac{\mu_t}{\sigma_k} + \mu \right) \frac{\partial k}{\partial x_j} \right] \\ &+ \frac{\mu_t}{\rho} \frac{\partial U_i}{\partial x_j} \left(\frac{\partial U_i}{\partial x_j} + \frac{\partial U_j}{\partial x_i} \right) - 2\nu \left(\frac{\partial k}{\partial x_j} \frac{\partial k}{\partial x_j} \right) - \epsilon \end{aligned} \quad (1)$$

$$\begin{aligned} \frac{D\epsilon}{Dt} &= \frac{1}{\rho} \frac{\partial}{\partial x_j} \left[\left(\frac{\mu_t}{\sigma_\epsilon} + \mu \right) \frac{\partial \epsilon}{\partial x_j} \right] \\ &+ C_1 \frac{\epsilon}{k} \frac{\mu_t}{\rho} \frac{\partial U_i}{\partial x_j} \left(\frac{\partial U_i}{\partial x_j} + \frac{\partial U_j}{\partial x_i} \right) \\ &- \frac{C_2 \epsilon^2}{k} - 2 \frac{\nu \mu_t}{\rho} \left(\frac{\partial^2 U_i}{\partial x_j \partial x_i} \frac{\partial^2 U_i}{\partial x_j \partial x_i} \right) \end{aligned} \quad (2)$$

Turbulent viscosity μ_t and the turbulent Reynolds number R_t are:

$$\mu_t = \frac{C_\mu \rho k^2}{\epsilon}, \quad R_t = \frac{k^2}{\nu \epsilon} \quad (3)$$

C_μ and C_2 vary with turbulent Reynolds number as

$$C_\mu = C_{\mu\infty} \exp \left[\frac{-2.5}{1 + R_t/50} \right] \quad (4)$$

$$C_2 = C_{2\infty} \exp \left[1 - 0.3 \exp(-R_t^2) \right] \quad (5)$$

the recommended constants are:

$$C_{\mu\infty} = 0.09, \quad C_1 = 1.44, \quad C_{2\infty} = 1.92, \quad \sigma_k = 1.0, \quad \sigma_\epsilon = 1.3$$

In parallel with the standard model, a variant of that, realizable k- ϵ model (Shih, Liou, Shabbir, Yang, & Zhu, 1995), which is also available in commercial software ANSYS-Fluent, is used to model turbulence; comparison of its results with those of standard model shows no significant differences. The used finite volume is a pressure-based algorithm although the Mach number reaches to around 2 and even more in throats. It is based on the recent extension and reformulation of ANSYS-Fluent to solve and operate for a wide range of flow conditions (Fluent, 2017). Pressure-velocity coupling is by SIMPLE Method.

The discretization schemes for all gradients are Green-Gauss node based. All flow equations together with turbulent kinetic energy and turbulent dissipation rate are solved using a second order upwind scheme; pressure equation is discretized second order.

Convergence criteria for continuity, momentum, k and epsilon equations are set to 1e-04, while that is 1e-09 for the energy equation.

The fluid is Methane with ideal gas density, c_p is a piecewise polynomial and its viscosity is 1.087e-05 kg/m.s. At the inlet, total pressure and temperature are given as boundary conditions, while the static pressure is given at the outlet. The hydraulic diameter is 0.08 m for the valve circular inlet and outlet and the turbulent intensity is set to 5%. Inlet total temperature is equal to 296 K correspond to test conditions. The walls are no-slip and adiabatic.

Some simplifications are considered in the solution. For example, the volumes occupied by the globe stems are ignored.

3. GRID ASSESSMENT

The structured boundary layer meshes near the walls together with in core flow unstructured meshes are used to mesh the flow domain. Figure 3 shows the meshed domain for GCV together with the grid at throats of both valves.

Grid independency checks are evaluated on parameters of outlet mass flow, velocity and pressure distribution at GCV throat. It is observed that the velocity distribution and its corresponding mass flow are not determinant for the grid independency, and the pressure distribution gives a more clear insight. Around 1400000 of meshes give the stable and unchanged results of the numerical method. The

grid qualities for the base load solution are minimum orthogonal quality of 0.23, maximum skewness of 0.932, and maximum aspect ratio of 37.4. The walls Y^+ maximum values are reported to less than 300, which show an acceptable fine mesh near the walls.

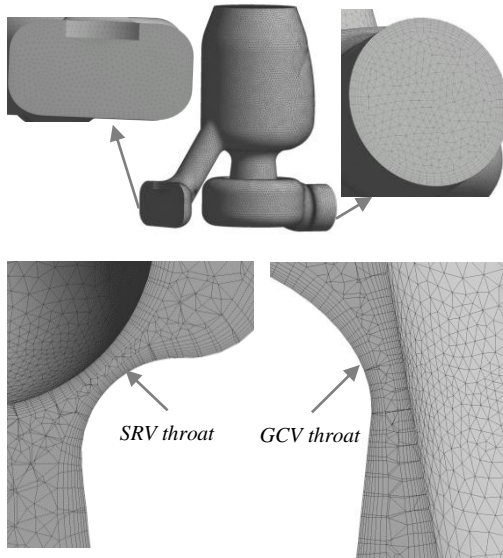


Fig. 3. The meshed domain of GCV and throats area.

4. VALIDATION AND GCV RESULTS

The GCV is the responsible part of the gas fuel control valve for a linear flow characteristic. Full speed no-load (FSNL) refers to a case during start-up in which the rotor speed reaches to nominal value but the load is zero. That corresponds to 18% opening of GCV. This is while the rated base load (RBL), with nominal speed and load, the GCV opening is 65%. Another condition is the rated peak load (RPL) in which the GCV stroke opens at 70%. One outermost condition is the peak load in cold day with 78% GCV opening. Table 1 and Fig. 4 compare obtained CFD results of GCV normalized mass flow for the above-mentioned cases with those of the site test data. For all the results, mass flow is normalized by reference values. The reference values refer to GCV ideal mass flow in cases of fully open with pressure ratio equal to 5, once with atmospheric pressure at valve outlet, and once again with the real rated pressure of turbine valve outlet. For FSNL, the area ratio of the valve outlet to the throat is approximately 22 while that is 5.5 in RBL. The C-D nozzle refers to the results of the converging-diverging nozzle flow with the same area ratios and conditions. In fact, the C-D nozzle results are a check for the valve results. The results show a good accuracy of the computational method.

Table 1 Comparison of CFD and site test data of GCV normalized mass flow

GCV opening	GCV mass flow		
	CFD results	Site test data	C-D nozzle
18% opening (FSNL)	0.199	0.187	0.209
65% opening (RBL)	0.720	0.729	0.774
70% opening (RPL)	0.781	0.777	0.830

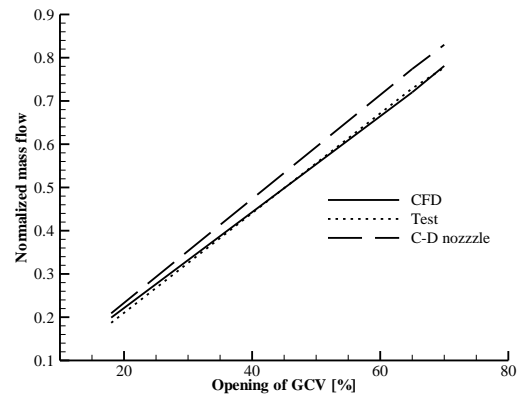


Fig. 4. Comparison of CFD, site test data and C-D nozzle of GCV normalized mass flow.

The flow domain is solved for various stroke positions of GCV by fixing the outlet pressure at atmospheric and increasing the inlet pressure to maintain the desired pressure ratio. The obtained results of normalized mass flow are shown in Fig. 5. Moreover, an equivalent mass flow, defined as $A = \dot{m} \sqrt{T_0} / P_0$ and shown in Fig. 6, the manufacturers occasionally refer to that and it emphasizes the linear behavior of mass flow with inlet total pressure for a wide range of valve pressure ratios. From the figure, it is obvious that for a constant total temperature test, the mass flow divided by total pressure first increases by increasing inlet total pressure (and hence pressure ratio) and then remains constant. This is completely in accordance with converging-diverging nozzle principles.

5. GCV AND SRV AS A COMPACT UNIT

As explained previously, fuel supply line pressure of the gas turbine sites are normally above 20 barg and in the time of turbine start-up (firing, warm-up and acceleration modes) the combustion chamber pressure is slightly more than atmospheric; this causes a large pressure ratio across the fuel control valve. Therefore, in firing when it needs a low fuel flow rate to the combustion chambers, the valve globe must be opened just a few percents of its total stroke (for example about 1 to 2%) and hence the flow control is a very difficult and costly task whit a single-container valve. The innovative design of the

double-container gas valve, including SRV followed by GCV in a compact unit, enables one to reduce pressure ratio on GCV through SRV. In this case, SRV maintains the appropriate pressure, P_2 , upstream to GCV. The pressure P_2 is normally determined through rotor speed. With this design, the minimum opening of GCV can be increased to 10 to 12%. Figure 7 shows GCV normalized mass flow values of 10% opening for various values of pressure ratios. Those are 0.018, 0.073 and 0.146 for PR= 2.5, 10 and 20, respectively. Therefore, in firing mode with 0.018 flow rate, the flame establishes in a safe manner.

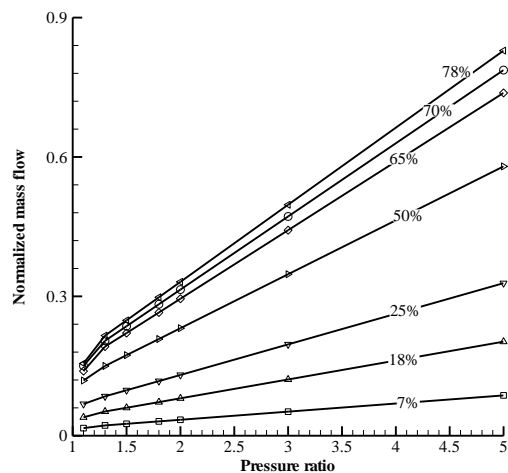


Fig. 5. GCV normalized mass flow with pressure ratio for various valve openings.

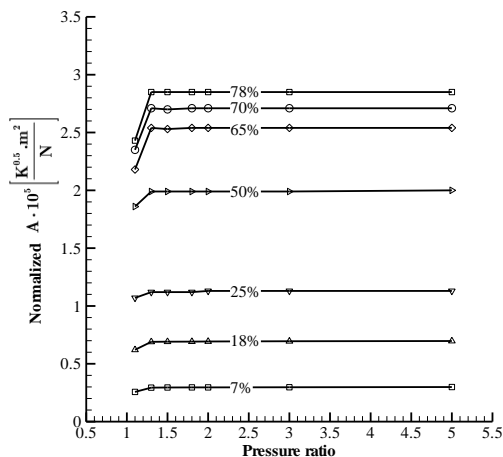


Fig. 6. GCV normalized mass flow with pressure ratio for various valve openings.

Six modes of the fuel valve operation are:

- 1) Firing: the rotor speed is 16% of nominal, the GCV opening is 17% of stroke, and the combustion pressure is slightly more than atmospheric,
- 2) Warm-up: with the same speed and combustion pressure as firing with 14% GCV opening,

- 3) Acceleration: with the same conditions of the previous two but 25% GCV opening,
- 4) FSNL: at nominal turbine speed and 18% GCV opening. In this case, the combustion pressure is 7.5 barg,
- 5) RBL: at 65% GCV opening and 12 barg combustion pressure,
- 6) RPL: at 70% GCV opening and 12.5 barg combustion pressure.

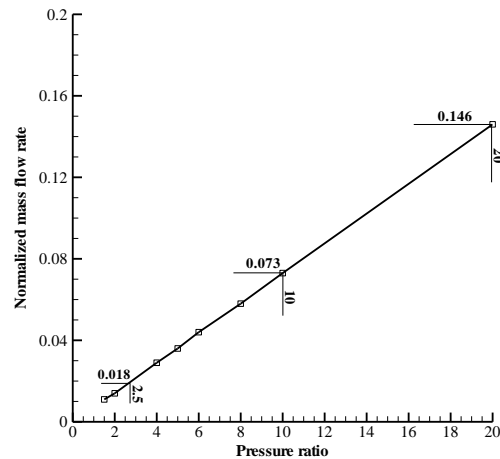


Fig. 7. Normalized mass flow with pressure ratio for 10% GCV opening.

The numerical results of the normalized mass flow of the fuel valve are compared in Table 2 with those of site test data for the above-mentioned modes of operation. For each case, SRV opening is given in the table. Up to FSNL, there observed a more tendency for the larger difference between CFD and site test data. This may be due to the real transient process of start-up, while its corresponding CFD is performed with a steady state assumption. The mass flow values are in accordance with the site data. The SRV stroke position gives an insight of its motion during turbine operation, and hence, the results are important in controlling system design. Figure 8 presents the filled contours of the static pressure of the valve. In Fig. 8, the different SRV stroke positions may not clearly be observed why the full stroke opening is just some millimeters compared to the whole size of the valve which is near one meter height. Figure 9 and Fig. 10 show the flow trajectories through the valve for two modes of FSNL and RBL. It clearly shows the vortical zone of the flow in above GCV plug.

A probable severe condition which occasionally happens in turbine sites is the decrease of gas supply line pressure to below the required value, i.e., 20+ bara (absolute pressure). It can be due to the for example winter cold climate or in a case of excessive demand for gas consumers. In this condition, the turbine speed is the same as nominal, and so, the controlling reference pressure between the SRV and GCV is the same as before. Therefore, the GCV is open at 65% and passes 0.719 mass

Table 2 Comparison of CFD and site test data of GCV and SRV mass flow

Operating mode	SRV opening [%]	GCV and SRV normalized mass flow	
		CFD results	Site test data
Firing	0.3	0.0199	0.0207
Warm-up	0.3	0.0199	0.0177
Acceleration	0.65	0.0395	0.0384
FSNL	3.5	0.199	0.187
RBL	12	0.719	0.728
RPL	13	0.780	0.779

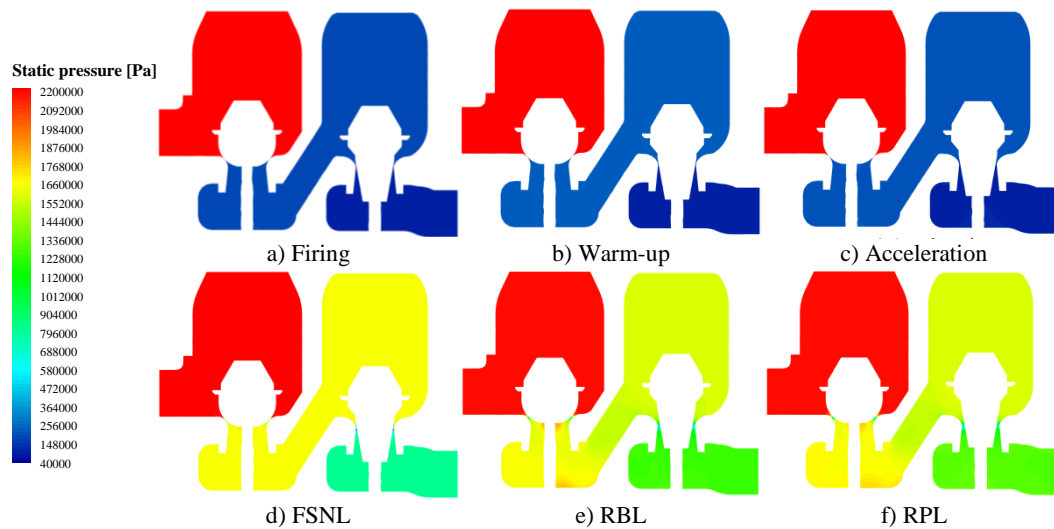


Fig. 8. Static pressure filled contour for various operating modes from firing to peak load.

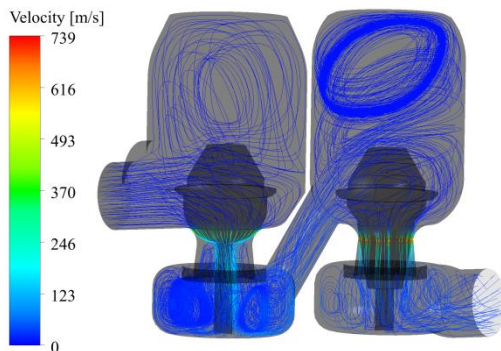


Fig. 9. Flow trajectories through the gas valve for FSNL operating mode.

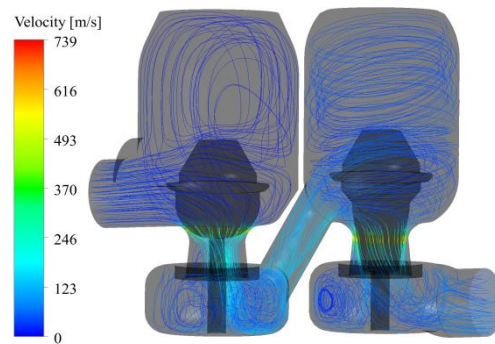


Fig. 10. Flow trajectories through the gas valve for RBL operating mode.

flowrate according to the value given in Table 2. It means the SRV opens to the extent that maintains the reference pressure as given controlling value. Table 3 gives the obtained results of SRV opening for various values of supply line pressures.

6. CONCLUSION

The present work is an attempt to numerically investigate the flow field through a double-container gas valve which controls fuel flow to the combustion chamber of various types of industrial gas turbines. The valve consists of two parts, a stop ratio valve (SRV) followed by a gas control valve

(GCV). Due to the fact that the gas supply line pressure of the turbine site is around 20+ bar, there exists a large pressure ratio across the valve in some modes of operation. Therefore, the proper control of the fuel flow through the valve, i.e., linear functional relation of mass flow with valve stroke position, cannot be maintained during turbine operation. SRV serves to keep the pressure at upstream the GCV equal to a reference value. This causes a small amount of pressure difference on GCV, and hence, a more manageable flow control. CFD analysis of the valve, both for SRV and GCV separately and as a compact unit, were presented. The numerical results of normalized mass flow

were compared with the turbine site test data and showed a good numerical estimation method. Moreover, contours of the static pressure and the flow trajectories were given for some modes of operation.

Table 3 SRV opening for various values of supply line pressure

Supply line pressure [bara]	SRV opening [%]
22	12
21	12.5
20	13
19	14
18	18
17	30
16.7	55
16.4	100

ACKNOWLEDGEMENTS

This research was conducted in MAPNA Turbine Company (TUGA), under the 42 MW gas turbine development program. The authors would like to express their gratitude to all contributors.

REFERENCES

- Amirante, R., G. Del Vescovo and A. Lippolis (2006a). Evaluation of the flow forces on an open centre directional control valve by means of a computational fluid dynamic analysis. *Energy Conversion and Management* 47(13), 1748-1760.
- Amirante, R., P. G. Moscatelli and L. A. Catalano (2007). Evaluation of the flow forces on a direct (single stage) proportional valve by means of a computational fluid dynamic analysis. *Energy Conversion and Management* 48(3), 942-953.
- Amirante, R., G. Del Vescovo and A. Lippolis (2006b). Flow forces analysis of an open center hydraulic directional control valve sliding spool. *Energy Conversion and Management* 47(1), 114-131.
- Beune, A., J. G. M. Kuerten and M. P. C. van Heumen (2012). CFD analysis with fluid-structure interaction of opening high-pressure safety valves. *Computers & Fluids* 64, 108-116.
- Chattopadhyay, H., A. Kundu, B. K. Saha and T. Gangopadhyay (2012). Analysis of flow structure inside a spool type pressure regulating valve. *Energy Conversion and Management* 53(1), 196-204.
- Davis, J. A. and M. Stewart (2002a). Predicting Globe Control Valve Performance—Part I: CFD Modeling. *Journal of Fluids Engineering* 124(3), 772-777.
- Davis, J. A. and M. Stewart (2002b). Predicting Globe Control Valve Performance—Part II: Experimental Verification. *Journal of Fluids Engineering* 124(3), 778-783.
- Fang, T., and S. Singh (2015). Predictions of Flow Separation at the Valve Seat for Steady-State Port-Flow Simulation. *Journal of Engineering for Gas Turbines and Power* 137(11), 111512-111517.
- Fluent, A. (2017). 18.1, Theory Guide, Ansys: Inc.
- Jin, Z. J., F. Q. Chen, J. Y. Qian, M. Zhang, L. L. Chen, F. Wang and Y. Fei (2016). Numerical analysis of flow and temperature characteristics in a high multi-stage pressure reducing valve for hydrogen refueling station. *International Journal of Hydrogen Energy* 41(12), 5559-5570.
- Jin, Z. j., Z. x. Gao, M. Zhang and J. y. Qian (2017). Pressure Drop Analysis of Pilot-Control Globe Valve With Different Structural Parameters. *Journal of Fluids Engineering* 139(9), 091102-091112.
- Lauder, B. E. and D. B. Spalding (1974). The numerical computation of turbulent flows. *Computer Methods in Applied Mechanics and Engineering* 3(2), 269-289.
- Lisowski, E., W. Czyżycki and J. Rajda (2013). Three dimensional CFD analysis and experimental test of flow force acting on the spool of solenoid operated directional control valve. *Energy Conversion and Management* 70, 220-229.
- Lisowski, E. and G. Filo (2016). CFD analysis of the characteristics of a proportional flow control valve with an innovative opening shape. *Energy Conversion and Management* 123, 15-28.
- Morita, R., F. Inada, M. Mori, K. Tezuka and Y. Tsujimoto (2007). CFD simulations and experiments of flow fluctuations around a steam control valve. *Journal of Fluids Engineering* 129(1), 48-54.
- Peng, Z. f., C.g. Sun, R. B. Yuan and P. Zhang (2012). The CFD analysis of main valve flow field and structural optimization for double-nozzle flapper servo valve. *Procedia Engineering* 31, 115-121.
- Qian, J. Y., L. Wei, Z. J. Jin, J. K. Wang, H. Zhang and A. L. Lu (2014). CFD analysis on the dynamic flow characteristics of the pilot-control globe valve. *Energy Conversion and Management* 87, 220-226.
- Qian, J. Y., L. Wei, M. Zhang, F. Q. Chen, L. L. Chen, W. K. Jiang and Z. J. Jin (2017). Flow rate analysis of compressible superheated steam through pressure reducing valves. *Energy* 135, 650-658.
- Saha, B. K., H. Chattopadhyay, P. B. Mandal and T. Gangopadhyay (2014). Dynamic simulation

- of a pressure regulating and shut-off valve. *Computers & Fluids*, 101, 233-240.
- Shih, T. H., W. W. Liou, A. Shabbir, Z. Yang and J. Zhu (1995). A new k- ϵ eddy viscosity model for high Reynolds number turbulent flows. *Computers & Fluids* 24(3), 227-238.
- Song, X., L. Cui, M. Cao, W. Cao, Y. Park and W. M. Dempster (2014). A CFD analysis of the dynamics of a direct-operated safety relief valve mounted on a pressure vessel. *Energy Conversion and Management* 81, 407-419.
- Wu, D., S. Li and P. Wu (2015). CFD simulation of flow-pressure characteristics of a pressure control valve for automotive fuel supply system. *Energy Conversion and Management* 101, 658-665.
- Zirak, S., H. Ebrahimi and A. R. Maissamy (2015). The required power of the MGT-40 gas turbine starter. *Energy Equipment and Systems* 3(2), 137-142.